agriculture

MDPI

Article

Effect of Fans' Placement on the Indoor Thermal Environment of Typical Tunnel-Ventilated Multi-Floor Pig Buildings Using Numerical Simulation

Xiaoshuai Wang [1], Mengbing Cao [1], Feiyue Hu [1], Qianying Yi [2], Thomas Amon [2,3], David Janke [3], Tian Xie [4], Guoqiang Zhang [5] and Kaiying Wang [1,*]

[1] College of Biosystems Engineering and Food Science, Zhejiang University, Hangzhou 310058, China; xiaoshuai.wang@zju.edu.cn (X.W.); mengbing.cao@zju.edu.cn (M.C.); hufeiyue@zju.edu.cn (F.H.)
[2] Department of Engineering for Livestock Management, Leibniz Institute for Agricultural Engineering and Bioeconomy (ATB), Max-Eyth-Allee 100, 14469 Potsdam, Germany; qyi@atb-potsdam.de (Q.Y.); tamon@atb-potsdam.de (T.A.)
[3] Department of Veterinary Medicine, Institute of Animal Hygiene and Environmental Health, Free University Berlin, Robert-von-Ostertag-Str. 7–13, 14163 Berlin, Germany; djanke@atb-potsdam.de
[4] Qingdao Big Herdsman Machinery Co., Ltd., Qingdao 266000, China; tian_xie123@163.com
[5] Department of Engineering, Aarhus University, Inge Lehmanns Gade 10, 8000 Aarhus, Denmark; guoqiang.zhang@cae.au.dk
* Correspondence: zjuwky@zju.edu.cn

Abstract: An increasing number of large pig farms are being built in multi-floor pig buildings (MFPBs) in China. Currently, the ventilation system of MFPB varies greatly and lacks common standards. This work aims to compare the ventilation performance of three popular MFPB types with different placement of fans using the Computational Fluid Dynamics (CFD) technique. After being validated with field-measured data, the CFD models were extended to simulate the air velocity, air temperature, humidity, and effective temperature of the three MFPBs. The simulation results showed that the ventilation rate of the building with outflowing openings in the endwall and fans installed on the top of the shaft was approximately 25% less than the two buildings with fans installed on each floor. The ventilation rate of each floor increased from the first to the top floor for both buildings with a shaft, while no significant difference was observed in the building without a shaft. Increasing the shaft's width could mitigate the variation in the ventilation rate of each floor. The effective temperature distribution at the animal level was consistent with the air velocity distribution. Therefore, in terms of the indoor environmental condition, the fans were recommended to be installed separately on each floor.

Keywords: airflow pattern; effective temperature; numerical evaluation; ventilation rate; shaft's width

Citation: Wang, X.; Cao, M.; Hu, F.; Yi, Q.; Amon, T.; Janke, D.; Xie, T.; Zhang, G.; Wang, K. Effect of Fans' Placement on the Indoor Thermal Environment of Typical Tunnel-Ventilated Multi-Floor Pig Buildings Using Numerical Simulation. *Agriculture* **2022**, *12*, 891. https://doi.org/10.3390/agriculture12060891

Academic Editor: Brad Ridoutt

Received: 14 May 2022
Accepted: 16 June 2022
Published: 20 June 2022

1. Introduction

The outbreaks of African swine fever (ASF) in China have wiped out many small-scale pig farms with conventional one-floor buildings since 2018, whose facilities were outdated and bio-safety was poor. To fill the demand gap for pork, the multi-floor pig building (MFPB) was proposed by many pig building designers with the advantage of increased land-use efficiency, especially with the constantly increasing land-use cost in China and the improved bio-safety management with the development of advanced facilities and management systems [1]. Since its first advent in China, MFPB has been widely built in many provinces, particularly in southeastern China, which is covered by hills and mountains. As a new type of animal building, a variety of designs emerged but were accompanied by debates in the industry about the optimal design due to the lack of recommendations for the construction and corresponding management of MFPB. Designers championed their designs based on many perspectives, including bio-safety, energy-saving,

indoor environmental control, and polluted gas removal. However, little consensus on the optimal design has been reached without evidence-based data.

For any commercial pig building, the indoor environmental condition is one of the most important factors affecting the health, performance, and behavior of pigs, as well as the quantity and quality of the pork [2,3]. To perform a comfortable living environment, ventilation is the most common and efficient way, which could replace the hot, humid, and polluted indoor air with fresh air [4,5]. Due to the importance of ventilation to pig production, studies have been conducted to evaluate the ventilation performance in MFPBs. Wang et al. firstly assessed the effect of floor numbers (ranging from 6-floor to 10-floor) and shaft width (20 m and 30 m) on the ventilation performance for a specific type of MFPB using numerical simulations [1]. According to the simulated results, they concluded that an increasing floor number negatively affected the ventilation rates of the MFPB and increasing the width of the shaft benefits the ventilation rates of the MFPB. However, they solely compared ventilation rate and airflow distribution across floors in the MFPB. As is well-known, thermal comfort is determined by many environmental parameters including air velocity, air temperature, relative humidity, etc. It is necessary to evaluate the distribution of air temperature, relative humidity as well as the effective temperature of pigs in the MFPB. Gao et al. reported differences in air temperature and relative humidity among floors inside four identical seven-floor pig buildings and stated that the differences in stocking density of each floor and the corresponding size/age of pigs mainly accounted for the environmental differences [6].

According to our best knowledge, limited studies were available in the literature. The aforementioned studies were the only two peer-reviewed publications, and both of them focused on the indoor environmental condition in a certain type of MFPBs [1,6]. As stated previously, many different types of MFPBs have been built recently, and the major differences among them are the existence of a shaft and the placement of exhausting fans. The shaft was expected to not only reduce the odor nuisance to neighbors but reduce the internal transmission of pathogens among floors. As a key component of the mechanical ventilation system, the exhausting fans can directly affect the indoor environmental conditions, and ventilation rate in particular [7]. Currently, there are many strategies for the placement of fans in the MFPBs. The different placement of exhausting fans would likely result in different ventilation performances, particularly in ventilation rate and indoor thermal environment. However, no systematic evaluation of the effect of the placement of exhausting fans on the ventilation rate and the indoor thermal environmental condition in the typical MFPBs has been done. To figure out the effect, a systematical comparison of the ventilation performance (ventilation rate among floors, indoor airflow pattern, thermal condition) of MFPBs with different placements of the bank of exhausting fans was necessary, which could not only provide a deep understanding of the ventilation performance in each typical type of MFPB but also offer a solid opinion on the aforementioned argument in the industry.

To perform such an evaluation, researchers can conduct several field experiments with different types of MFPBs. However, field experiments are expensive, labor intensive, and time consuming, let alone the difficulty in getting permission from AFOs under the ongoing ASF epidemic. Note that, due to the strict and mandatory hygiene precautions, it is almost impossible to conduct a field experiment in commercial pig buildings in China currently. In addition, a reasonable comparison of the ventilation performance in different types of MFPBs required a comparable layout of indoor structure (pen size, feeders, etc.), stocking density, and pig size because all the aforementioned factors would affect the ventilation performance. Thus, it would be very difficult to achieve the comparison using a series of field measurements. Alternatively, the Computational Fluid Dynamics (CFD) simulation technique has been widely used in the evaluation of the indoor environmental condition and the ventilation system in many animal buildings [1,8–14]. All the studies proved that CFD simulation is a feasible, fast, and parameter-controllable way to conduct such evaluation. Thus, the CFD simulation method was adopted in this study.

Therefore, the objective of this study is to evaluate the difference in the ventilation rate and the indoor thermal environmental condition of the three typical types of MFPBs by using CFD simulations. The results could provide useful information for the industry and the MFPB designers from the ventilation perspective.

2. Materials and Methods

Assumption:

This study was based on the following assumptions:

- The ambient environmental condition was stable during the field measurement. The blockage effect of the steel posts and feeding troughs on the airflow was not considered due to the limited effect compared with pigs.
- To consider the blockage effect of the pigs on the air movement, all the CFD simulations in this study were based on a certain stocking density for 50 kg pigs.

2.1. Description of the Three MFPBs

Generally, there are three typical types of MFPB, as shown in Figure 1. They all adopt a tunnel ventilation system, in which the wetpads serve as air inlets. The differences among these three types are the placement of fans and the existence of the shaft. The first type of MFPB (referred to as B1) simply stacks the conventional one-floor pig barn into a multi-floor pig barn (Figure 1a). The fans are installed at the opposite endwall to the inlet, and no shaft is constructed. The second type of MFPB (referred to as B2) has a shaft surrounding the exhausting fans (Figure 1b), and the outgoing air from each floor was released from the top of the shaft. In B1 and B2, the wet pads and exhausted fans were installed at the opposite endwalls on each floor, serving as air inlets and outlets, respectively. The difference between B1 and B2 was the existence of a shaft. The third type of MFPB (referred to as B3) is similar to B2, except for the location of the fans installed (Figure 1c). The exhaust fans are installed together in three levels (L1-3) at the top part of a higher shaft in B3, while the fans are installed at the endwall on each floor in B1 and B2. There are four openings in the endwall of each floor. Both B2 and B3 have a shaft, which collects polluted air and releases the air from the top of the building before the pollutants such as NH_3, H_2S, odors, and particulate matter, are completely removed.

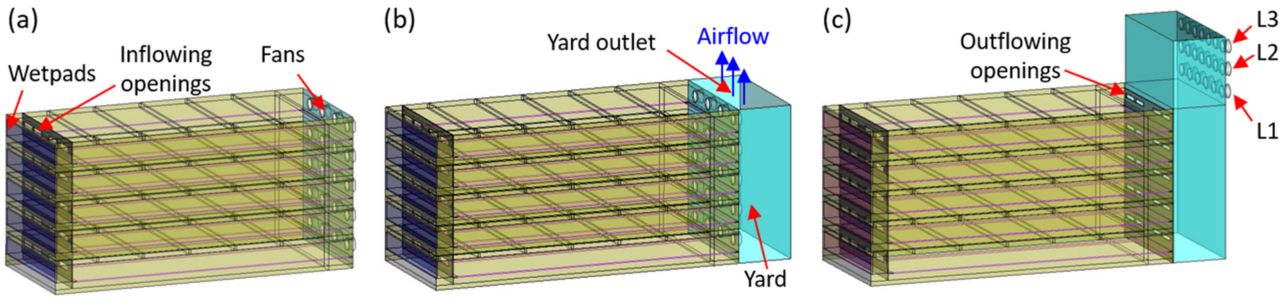

Figure 1. Sketches of the three different MFPBs: (**a**) B1, (**b**) B2, and (**c**) B3. The three levels of the fans in B3 were indicated as L1, L2, and L3.

For better comparison, the components affecting ventilation, including the layout of the pens, the size of animal-occupied zones, the number and type of the exhaust fans, the size and depth of wetpads, and the geometry of the inflowing openings, were all kept the same in this study. In terms of the installation of the twenty identical fans, four identical fans were installed at the endwall on each floor in both B1 and B2, as illustrated in Figure 1a,b, and six, seven, and seven identical fans were installed at the L1, L2, and L3, respectively, in B3 in Figure 1c.

2.2. CFD Modeling

2.2.1. Computational Domain and Grid Distribution

Considering the structural characteristics of MFPBs, only a unit of each MFPB was modeled for the simulation. By doing so, the simulation cost (time and computational effort) could be greatly reduced without great sacrifice of the accuracy of the simulation. Figure 2a–c shows the computational domains and the corresponding geometric information for the three MFPBs, which consist of a building unit and the ambient domain. Solidworks (Dassault Systems S.A. France) was used for modeling the computational domain.

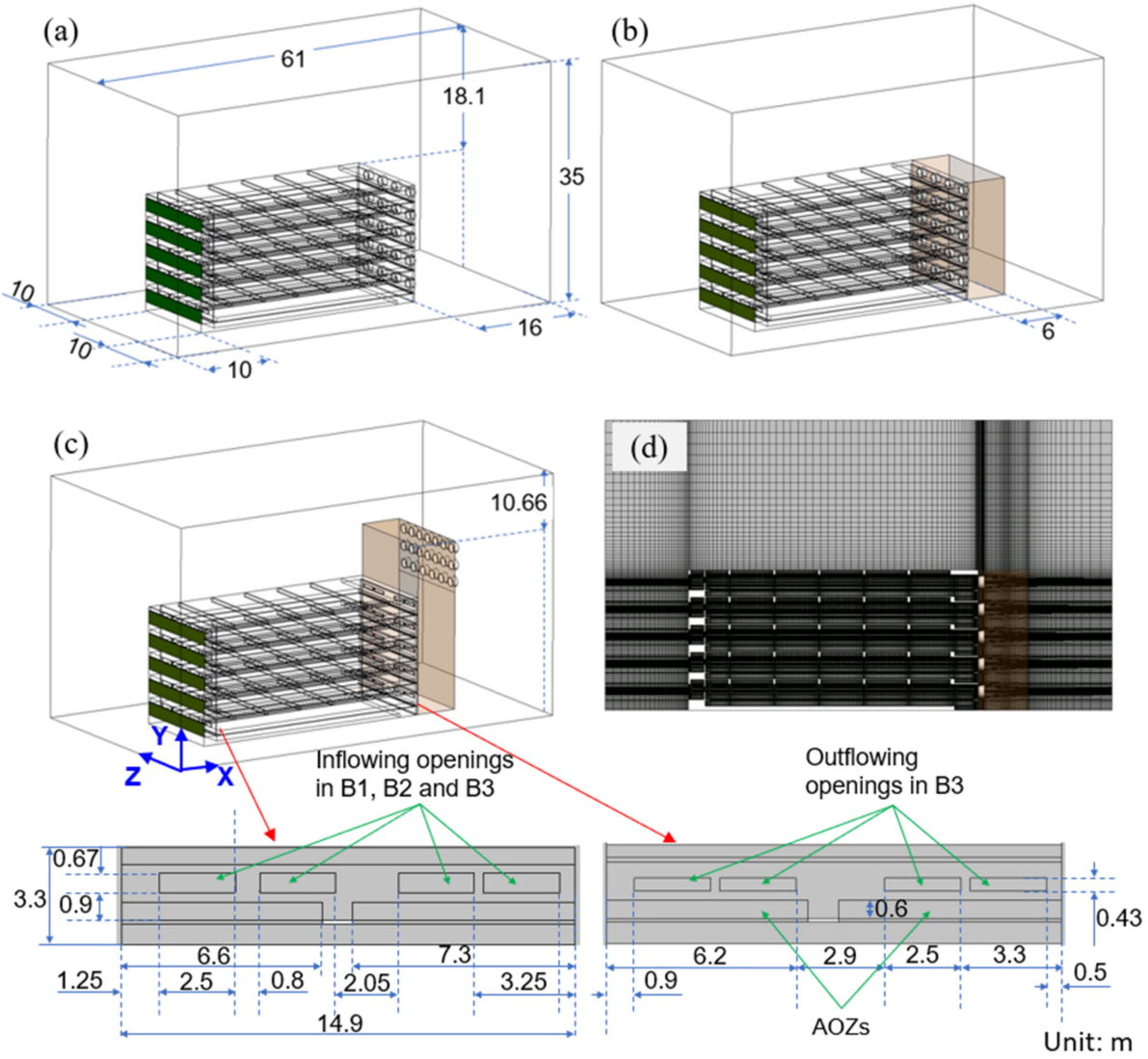

Figure 2. (**a**–**c**) Computational domain including the MFPBs (B1, B2, and B3, respectively) and the corresponding expanded domain and the dimensions of the inflowing and outflowing openings. (**d**) The mesh distribution of a virtual vertical plane of B2.

The structural (hexahedral) meshing strategy was applied to ensure the mesh was of good quality, in which the growth ratios of the grid were set to be less than 1.25. To ensure that the simulated results were independent of the grid resolution, a grid-independent test was conducted with four levels of the grid resolution. The steps of the grid independency test and the strategy of the meshing were consistent with the one introduced in the previously published paper [1]. Figure 2d shows the selected mesh distribution strategy (using B2 as an example, 17,814,020 hexahedral cells in total), and the

mesh distributions for the rest two buildings were similar. The meshing procedure was done using Ansys ICEM (ANSYS, Inc., Canonsburg, PA, USA).

2.2.2. Governing Equation and Simulation Scheme

In this study, the motion of airflow was modeled using the Reynolds-averaged Navier-Stokes (RANS) approach with the general governing equation expressed as Equation (1) [15]:

$$div(\rho \Phi u) = div(\Gamma_\Phi \, grad \Phi) + S_\Phi \quad (1)$$

where ρ is density, kg m^{-3}; u is the velocity, m s^{-1}; Φ represents the common variables of interest, i.e., velocity, m s^{-1}, turbulent kinetic energy, m^2 s^{-2}, and its dissipation rate, m^2 s^{-3}; Γ_Φ is the transport coefficient dependent on Φ, and S_Φ is the source term dependent on Φ.

The governing equation was implemented in the commercial CFD code ANSYS FLUENT (ANSYS, Inc. USA), and discretized by the SIMPLE (Semi-Implicit Method for Pressure-Linked Equations) scheme. Second-order upwind discretization was selected for momentum, turbulent kinetic energy (k), and specific dissipation rate (ε). The realizable k-ε turbulence model was selected in this study since previous investigations have shown that it can better replicate the airflow inside the livestock buildings [16–18]. Enhanced wall treatment was enabled in the simulation, and the area-weighted average values of Y+ in all the simulation cases were kept within the required range (Y+ > 30).

Regarding convergence criteria, the absolute residuals of continuity, velocity, k, and ε should all be less than 1×10^{-4}, and the monitored value (the area-averaged air velocity at the cross-sectional virtual plane of each cone of a randomly selected fan) needed to be stable (relative difference of less than 0.5% within 100 iterations).

2.2.3. Simplifications of the Animal-Occupied Zone

The simplification of the animal-occupied zone (AOZ) included the simplifications of airflow, heat generation, and moisture generation inside the AOZ. Since the airflow underwent a pressure drop when passing through the AOZ, porous media volume (PMV) treatment was applied to simplify the effects of the pigs on the airflow in the AOZ in the CFD model. By doing so, the meshing and computational load could both be greatly reduced with an acceptable difference in results. Generally, the pressure drops across a PMV can be described by the sum of the viscous loss and inertial loss [19]:

$$\Delta P_x / \Delta l_x = -\left(D_x \mu v + \frac{1}{2} C_x \rho v^2 \right) \quad (2)$$

where $\Delta P_x / \Delta l_x$ is the pressure drop per unit length for x-direction, Pa m^{-1}; D_x and C_x are prescribed matrices for viscous and inertial resistance coefficients, m^{-1} and m^{-1}, respectively; v is inlet air velocity, m s^{-1}; μ is the dynamic viscosity of air, N s m^{-2}; and ρ is air density, kg m^{-3}.

The viscous and inertial resistance coefficients were adopted from a published study [20], in which the determination of the airflow resistance coefficients was based on an assumed fattening pig weight of 50 kg and the stocking density was 0.73 m^2 head^{-1}. Considering the layout of the pens in the MFPB, the dimensions of AOZs were 31 m long × 7.3 m wide × 0.6 m high and 31 m long × 6.6 m wide × 0.6 m, respectively. Note that, the AOZ height of 0.6 m was determined according to the relationship between pig weight and the corresponding body height [21], expressed as Height = (Body Weight)$^{0.33}$.

Pigs generate both sensible and latent heat. The total heat (Φ_{tot}, W), sensible heat (Φ_s, W), and latent heat (Φ_l, W) produced per fattening pig were calculated from Equations (3)–(5), respectively [22].

$$\Phi_{tot} = \frac{1000 + 12 \times (20 - Ta)}{1000} \left\{ 5.09 m^{0.75} + [1 - (0.47 + 0.003m)] \left[n \times 5.09 m^{0.75} - 5.09 m^{0.75} \right] \right\} \quad (3)$$

$$\Phi_s = 0.62\Phi_{tot} - 1.15 \times 10^{-7} \times Ta^6 \quad (4)$$

$$\Phi_l = \Phi_{tot} - \Phi_s \quad (5)$$

where Φ_{tot}, $\Phi_{s,}$ and Φ_l represent the total, sensible, and latent heat production by fattening pig, respectively, all in W; *Ta* represents air temperature, °C; m represents the weight of fattening pig, kg, in this study, we assumed the pig weight m = 50 kg; and n represents the daily feed energy intake, for 50 kg fattening pig, n = 3.52 [22].

To model the process of heat and moisture generation in the AOZ by the pigs, the heat and moisture generation rates, as source terms in the CFD model, were calculated as shown in Equations (6) and (7), respectively, and compiled into the model by means of so-called user-defined functions (UDFs).

$$Q_s = \Phi_s \times \frac{N}{V} \quad (6)$$

$$M_l = \frac{\Phi_l}{r} \times \frac{N}{V} \quad (7)$$

where Q_s represents the sensible heat source generation rate, W m^{-3}; N represents the number of pigs on each floor; V represents the total porous media volume of AOZ on each floor, m^3; M_l represents the moisture generation rate, kg $s^{-1}{\cdot}m^{-3}$; r represents the latent heat of vaporization, kJ kg^{-1}.

2.2.4. Simplifications of Wetpad and Slatted Floor

When hot and dry air passes through the wetpads, it would be wetted and cooled [23]. Therefore, the wetpad could be deemed as a heat sink and moisture source in the PVM modeling. However, this study focused on the ventilation performance and corresponding indoor environmental conditions inside the MFPBs rather than the performance of wetpad cooling. Therefore, the process of cooling by a wetpad was simplified by means of setting the incoming air temperature and relative humidity as the value when the ambient air passes the wetpad. In this study, the outside air with 38.0 °C and 80.0% could be cooled to 35.1 °C and 96.7% when it passed through the wetpads with an assumed cooling efficiency of 85%, the temperature and relative humidity of the incoming air were set as 35.1 °C and 96.7%, respectively.

The airflow in the wetpad was simplified based on published data from a field measurement [24]. The detailed information for the determination of the two resistance coefficients could be found in our previous study [1]. Since no heat and moisture were generated from the slatted floor, only the simplifications of slatted floors were used to simplify the airflow. The setups for the viscous and inertial resistance coefficients of the slatted floor were adopted from a published study [20], in which the geometry of the slatted floor was comparable with the one in this study. Table 1 lists the viscous and inertial resistance coefficients of AOZ, slatted floor, and wetpads.

Table 1. The setups of PMM for AOZ, slatted floor, and wetpads.

Item	R_1, m^{-1}			R_2, m^{-2}			Moisture Generation Rate, g/m^3	Heat Generation Rate, W/m^3
	x	y	z	x	y	z		
AOZ	0.4	0.4	0.4	400	400	400	UDF	UDF
Slatted floors	80	80	-	15,000	15,000	-	-	-
Wetpads	11.06	-	-	182,754	-	-	-	-

2.2.5. Simplification of Fans

An exhaust fan could produce a pressure jump when operating, and the pressure jump is dependent on the air velocity passing through the fan's orifice. To properly model the fans on the endwalls, Fan, a type of boundary condition in Fluent, was selected in the CFD model. The fan modeled in this study was based on the fan used in the field experimental

MFPB. The orifice and blade diameter of the fan (Qingdao Big Herdsman, EF51FC01) were 130.5 and 129.0 cm, respectively. The pressure jump in the CFD model would automatically be modified according to the passing through air velocity, following Equation (8), which was determined by the performance curve based on the final report by Bess Lab, UIUC [25], with R^2 of 0.99.

$$\Delta P = -0.2562u^3 + 3.3931u^2 - 19.88u + 101.96 \quad (8)$$

where the ΔP denotes the pressure jump of a fan, Pa; and u is the air velocity passing through the fan, m s^{-1}.

2.3. Field Experiment for CFD Model Validation

Field measurements were carried out in a newly built five-floor pig building (Figure 3a) located in Kaijiang, Sichuan province, China on 27 May 2021. The first floor of the pig building was used for finishing; the second and third floors were used for piglet nursery; and the fourth and fifth floors were used for farrowing. The pig building is similar to the B3 (as illustrated in Figure 1), in which the width of the shaft was 6 m. There were no pigs raised in the building during the field measurement. Additionally, the slatted floor in the pens, automatic feeding system, and rope manure scraper were applied in the tested MFPB.

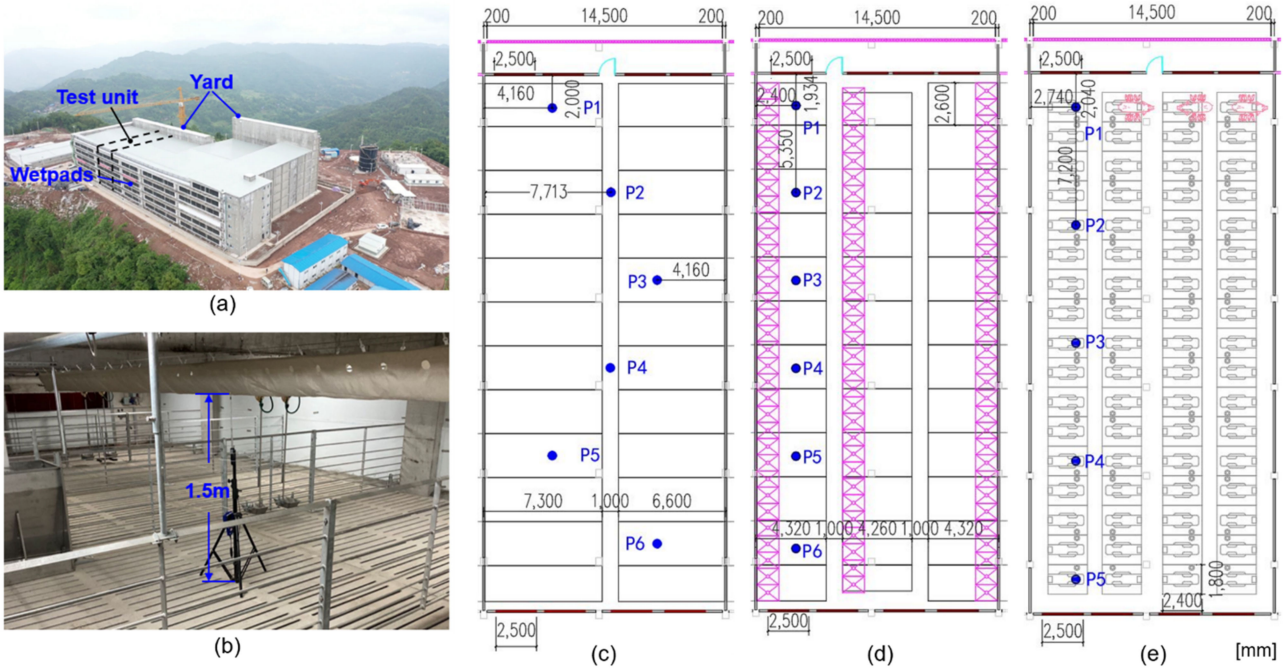

Figure 3. Photos of the (**a**) tested MFPB and (**b**) measurement sensor. The layout of the measurement locations at (**c**) 1st floor (finishing room), (**d**) 2nd and 3rd floor (nursery room), and (**e**) 4th and 5th floor (farrowing room) in the raising part in tested MFPB (marked as the blue dot). The shaft part was omitted in (**c**–**e**).

The field measurement lasted 7 h, from 8:30 am to 2:30 pm. Environmental parameters, including air temperature (Ta), relative humidity (RH), and air velocity (v), were measured using portable hot-wire anemometers (VelociCalc® Multi-Function Ventilation Meter 9565-A, TSI, Shoreview, Minnesota, USA). The measuring accuracies of Ta, RH, and v were ±0.3 °C, ±3%, and ±0.015 m s^{-1}, respectively. Each floor had 5 or 6 measuring locations with a height of 1.5 m from the slatted floor and the layout of the measuring locations was listed in Figure 3c–e. The measurement on each floor was conducted simultaneously by 5 or 6 anemometers. The three parameters (Ta, RH, and v) were recorded every 5 s for 40 min at each location. Approximate 450 valid samples were collected at each measurement location. The measurement started from the first floor.

2.4. Data Processing and Analysis

2.4.1. Ventilation Rate

The ventilation rate, VR, was selected as the comparing parameter in this study to quantitatively evaluated the difference between floors and MFPBs. The ventilation rate of each floor was calculated using VR = $v_{ave\_x} \times A$, where the v_{ave_x} represents the averaged velocities in the x-direction at the cross-section of the fan cones for B1 and B2 and the outflowing openings for B3 (which were indicated in Figure 2c), and the A denotes the cross-sectional area of either the fan cones or the openings.

2.4.2. Thermal Comfort Index

In this study, the Effective Temperature (ET, Equation (9)) was used to evaluate the thermal environmental conditions because ET incorporates not only the effect of local air temperature and relative humidity but also the effect of local air velocity on the thermal comfort of pigs [26].

$$ET = Ta - 0.0015Ta(RH - 50) - (42 - Ta)\left(u^{0.66} - 0.2^{0.66}\right) \quad (9)$$

where ET represents the effective temperature for pig, °C; RH denotes the relative humidity, %; and u denotes the air velocity, m/s.

In addition, the field-measured and simulated data were processed and analyzed using Office Excel. Plots illustrated in this study were drawn using either CFD Post (ANSYS, Inc. USA) or Origin 2020 (OriginLab Corporation, Northampton, MA, USA).

3. Results and Discussion

3.1. CFD Model Validation

To validate the CFD model, the simulated air velocities were compared with the field measured ones because the airflow acted the most important role in the ventilation performance of the tunnel ventilation system. Note that, since no pig was raised in the building during the experiment, there was no heat source or moisture source in the CFD model for the model validation; therefore, the indoor air temperature and relative humidity at the measuring points were not compared with the simulated ones in this study. Figure 4a showed the comparison of the measured and simulated air velocities at each measuring location, in which the measured air velocities were summarized in the box plot, and the corresponding simulated ones were plotted in scatter (marked as blue dots). Most of the simulated velocities were close to the corresponding measured ones, except for the measuring points F2P2 (F2P2 represents the second measuring point on the second floor), F3P2, and F4P2, where the simulated velocities were greater than the measured ones. The great air velocity gradient in the second measuring location accounted for the differences in the measured and simulated air velocities at F2P2, F3P2, and F4P2 because the measuring points F2P2, F3P2, and F4P2 were all located in the air jet plume. Besides, the variations of both the measured and simulated air velocities were similar. Therefore, the CFD model developed in this study could be deemed valid.

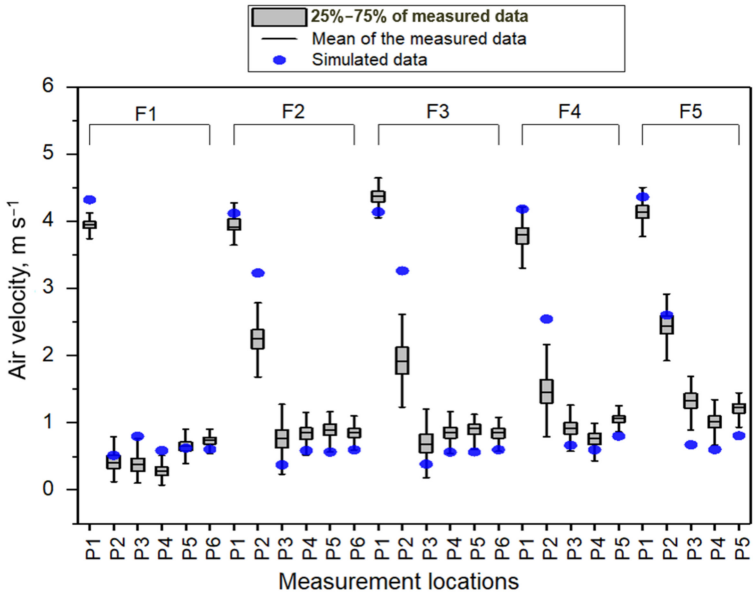

Figure 4. Comparison between field-measured and simulated data. The measured air velocity at each floor and each measuring point were displayed using boxplot, the corresponding simulated air velocities were plotted using blue dots. F1, F2, F3, F4, and F5 denote the 1st, 2nd, 3rd, 4th, and 5th floors, respectively.

3.2. Ventilation Rates in MFPBs

Figure 5 showed the ventilation rate on each floor of all three types of MFPB. For the ventilation rates in B1, no significant difference was observed among each floor with an average ventilation rate of 106.66 $\times$ 10^3 m^3 h^{-1} because the ventilation system on each floor was relatively independent in B1. The ventilation rates in B2 increased gradually from the first floor (103.58 $\times$ 10^3 m^3 h^{-1}) to the fifth floor (107.81 $\times$ 10^3 m^3 h^{-1}). The relative difference between the first floor and fifth floor was 3.9%. The variation tendency of the ventilation rates in B2 was consistent with the previously published study [1]. Compared with the ventilation rates in B1, the increase in the ventilation rates from the bottom floor to the top floor in B2 can be attributed to the existence of the shaft in B2, in which the airflow-induced vertical pressure gradient in the shaft affected the performance of the exhausting fans.

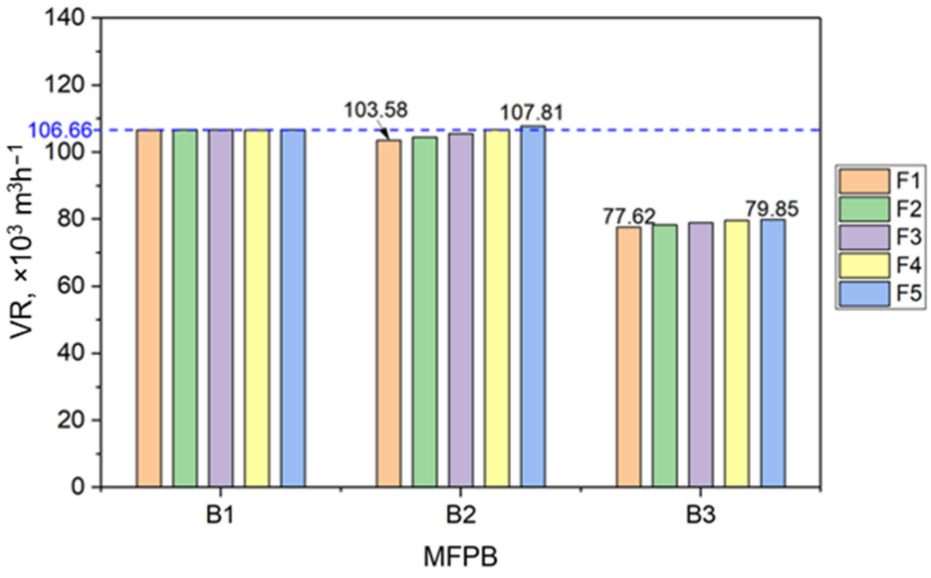

Figure 5. Ventilation rate at each floor of the three five-floor pig buildings.

For B3, the ventilation rates were around 25% less than the ventilation rates of B1 and B2. The openings in the endwall (as indicated in Figure 1c) accounted for the difference in the ventilation rate. Theoretically, these openings could be deemed as orifices, when the air passes through the openings, its pressure builds up slightly upstream of the openings. Therefore, enlarging the size of the outflowing openings could decrease the pressure drop when airflow passes through the openings, resulting in an increase in the ventilation rates. Additionally, similar to the variation of ventilation rate at each floor in B2, the ventilation rate at each floor in B3 increased gradually from 77.62 $\times$ 10^3 m^3 h^{-1} on the first floor to 79.85 $\times$ 10^3 m^3 h^{-1} on the fifth floor, indicating that the pressure difference in the shaft also affected the ventilation rate of each floor.

3.3. Effect of Shaft Width on Ventilation Rates in MFPBs

As stated previously that the shaft contributed to the variation of the ventilation rates from floor to floor. Additional simulations with three levels of the shaft's widths, i.e., 4 m, 6 m, and 8 m, were simulated to evaluate the shaft's width effect on the ventilation performance of B2 and B3. The buildings with a six-meter-wide shaft were deemed practical cases. Figure 6a showed the ventilation rate of each floor of B2 and B3 with different widths of the shaft. The relative difference in ventilation rate between the bottom floor and the top floor decreased as the width of the shaft increased for both types of buildings (Figure 6a), indicating that prolonging the width of the shaft could narrow the difference in ventilation rates between the bottom and top floor. Similar results were reported by Wang et al. [1]. This phenomenon could be attributed to the pressure difference in the shaft with different shaft widths. Figure 6b illustrated the pressure profile inside the shaft in B2 and B3 with the three different shaft widths and the pressure decreased along with the height increase from the bottom to the top of the shaft. Generally, given a similar ventilation rate, the smaller sectional area of the shaft (because of the smaller width of the shaft) would cause a greater sectional averaged air velocity, resulting in a greater pressure gradient field inside the shaft. The difference in the local pressure close to the fans affected the fans' ventilation performance in B2 and the difference in the local pressure close to the outflowing openings among floors also affect the ventilation rate that passed through the openings in B3.

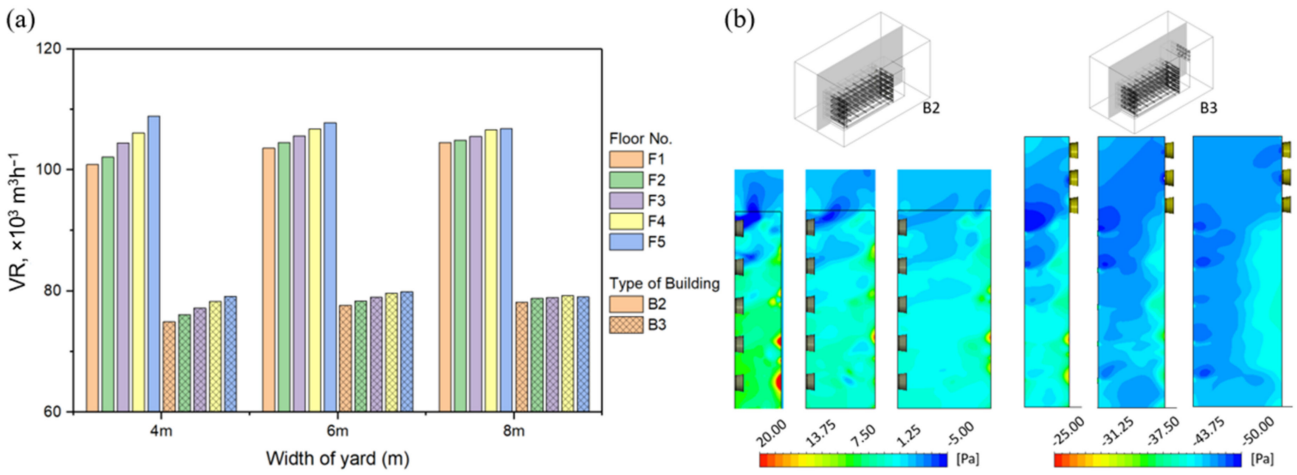

Figure 6. Ventilation rate at each floor (**a**) and contours of the pressure profile in B2 and B3 (**b**) with 4 m, 6 m, and 8 m-wide shaft.

3.4. Airflow Pattern in MFPBs

Figure 7 showed the contours of air velocity at two virtual planes with a height of 0.3 and 1.3 m from the slatted floor on the third floor and the air velocity at the vertical plane with a distance of 4.6 m to the left sidewall in all the three MFPBs. As can be seen, the airflow patterns in the raising part for all the three MFPBs were similar, which can be attributed to the similar ventilation components and organizations (inlets on one endwall

and outlets on the opposite endwall) used in these three buildings. In each of Figure 7a–c, a dark blue area was observed at the pens close to the inflowing openings, indicating that airflow in the zone was stagnant with an air velocity of less than 0.2 m s^{-1}. Such a stagnant zone occurred because the inflowing openings were set too high (0.9 m from the floor, 0.3 m higher than the height of the animal-occupied zone). According to Figure 7d–f, the air velocities from the inlet opening at the height of 1.3 m from the floor in both B1 and B2 were around 1 m s^{-1} greater than that in B3, indicating that the airflow rate in B3 could be smaller than those in B1 and B2. Comparing the air velocity at the two heights, the air velocity at AOZ was much less than the air velocity at the height of 1.3 m from the floor. For Figure 7g–i, the fresh air through the inflowing openings flew to the ceiling firstly, resulting in limited air movement and air exchange rate in the animal-occupied zone close to the inflowing openings. This phenomenon was consistent with the contours of air velocity illustrated in Figure 7a–c. Afterward, the airstream was deflected into the animal-occupied zone by the second ceiling joist. According to the contours, it can be observed that the air movement inside the AOZ was much smaller than that at the headspace. Based on the results, most fresh air flew from inlets to outlets through the headspace of the raising part instead of going through the AOZ, resulting in the limited air movement in the AOZ.

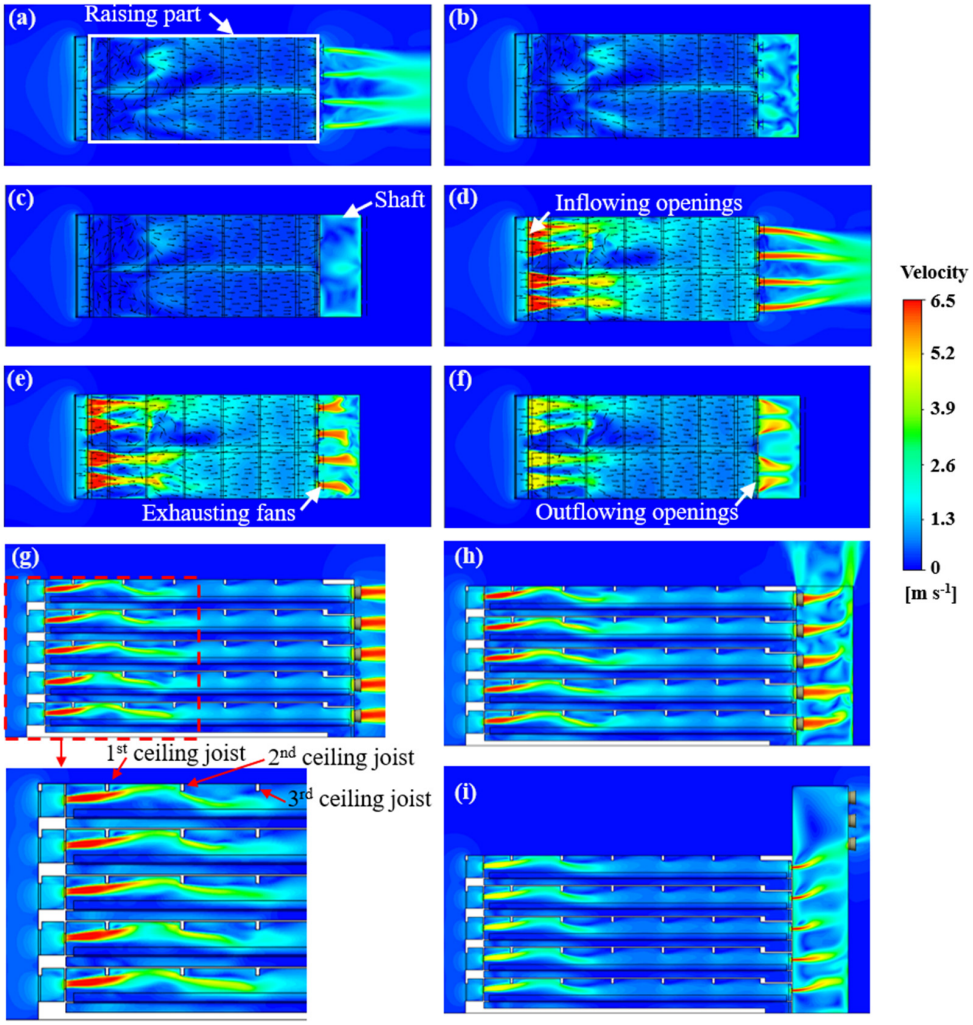

Figure 7. Contours of the air velocity and vector plots at planes with a height of 0.3 m (**a**–**c**) and 1.3 m (**d**–**f**) of B1, B2, and B3, respectively; Contours of the air velocity at the vertical plane with a distance from the left sidewall of 4.6 m (**g**–**i**) of B1, B2, and B3, respectively.

3.5. Thermal Conditions in MFPBs

Since effective temperature (ET) is a measure reflecting the local thermal environmental condition for the animal, the ET distribution at the animal level (0.3 m from the slatted floor) on the third floor in all three MFPBs was displayed in Figure 8. By doing so, the local thermal condition could be better illustrated than solely analyzing the local air temperature and relative humidity. According to Figure 8, the ET contours of B1 and B2 were similar because B1 and B2 had a similar ventilation rate for each floor and the corresponding airflow pattern. The ET contour of B3 was darker than those of B1 and B2, indicating that the ET in B3 was relatively higher (around 1–2 degrees higher) than those in B1 and B2. The lower ventilation rate in B3 accounted for the difference in ET among the buildings.

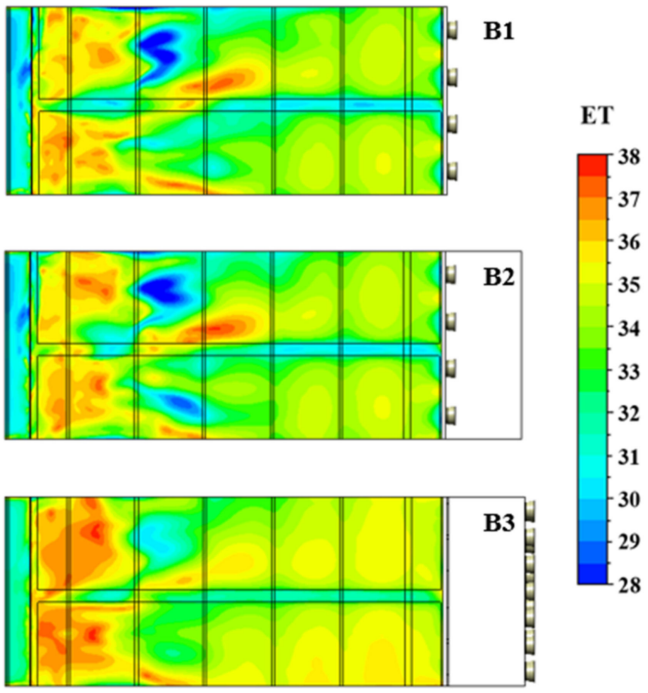

Figure 8. Contours of ET at the animal level (0.3 m from the slatted floor) on the 3rd floor in the three MFPBs.

The variation trends of ET from the inlet opening to the outflow opening at the animal level were similar for all three types of buildings. The ET in the area closed to the inlet openings was higher than in the rest of the area. The limited air movement in this area (as illustrated in Figure 7) contributed to this phenomenon. Given such a limited air exchange rate in this area, the moisture and heat generated by the animal would be accumulated. Interestingly, the pens next to the stagnant area were the coolest area in the entire raising unit, which could be attributed to the airflow pattern inside the buildings. As previously stated, the incoming cooling air was deflected from headspace to the animal-occupied zone by the second ceiling joist (as shown in Figure 7g). Therefore, the fresh cooled air in this area can be induced into the AOZ level and remove the heat and moisture. As the distance to the inlet openings increase, the value of ET increased as well.

According to results relating to the ventilation rate and effective temperature, we found that under the current ventilation system and components, there always were stagnant zones located closely to the inflowing openings. To improve the living environment in the AOZs, better mixing of the air between the higher and lower areas in the units should be aimed under current tunnel ventilation systems. Changing the vertical positions of both inflowing openings and the fans (in B1 and B2) and the outflowing openings (in B3) could be an option. Adding baffles or ceiling deflectors in the tunnel ventilated barn is also encouraged to attempt because baffles or deflectors could induce the fresh air from

headspace into AOZ and increase the local air exchange rate [14,27]. Besides, different ventilation systems with better air distribution performance, such as underfloor ventilation systems [28] and fiber duct air ventilation systems [8], could also be considered.

3.6. Limitations and Perspectives

According to the above findings and from the perspective of ventilation performance, the types of B1 and B2 were recommended rather than the type of B3 because, given the same number of fans, the ventilation rate of each floor in B1 and B2 would be greater than that of B3. In other words, to ensure an amount of ventilation rate similar to that in B1 and B2, more fans were required in B3, which would result in higher costs in construction, operation, and maintenance. The presumed advantage of the B3 was the ventilation rate at each floor could be controlled by modifying the size of the outflowing openings; however, such control of ventilation rate at each floor could also be achieved by adding an inverter fan at each floor instead.

In this study, we used the 50-kg pigs as an example for the evaluation of the ventilation rates and the indoor thermal environmental conditions under the three typical MFPBs. Due to different stocking densities and body weights, the results of the simulations might be different because the resistance coefficients of animal-occupied zones will be different. Because no additional data for the coefficients' setup was available, the published data with specific body weight and stocking density were applied. Additionally, the general qualitative findings, including the airflow pattern in each type of building, the variation tendency of the ventilation rates, the airflow patterns, and the effective temperature distributions were still valid. Future work could be focused on the simplification of the animal-occupied zone under different body weights and stocking densities, thus more scenarios could be investigated. Besides, the pollutant air dispersion under the three MFPBs should be investigated because as the emission height increase and the outflowing direction changes, the dispersion pattern would be different and the corresponding policy for the setback distance would be varied as well.

4. Conclusions

In this study, we evaluated the performance of the ventilation system in three popular types of MFPB. The ventilation rates among floors in the three MFPBs were simulated and compared. According to the results, we can conclude that the placement of the fans affects the performance of the ventilation system, particularly the ventilation rate. Placing the fans on the endwalls on each floor performed better than the one that placed all of the fans on the top of the shaft. Moreover, the shaft accounted for the difference in ventilation rate among floors. A wider shaft could narrow the relative difference in ventilation rate between the bottom floor and top floor. The height of openings and the ceiling joist contribute to the indoor airflow pattern, resulting in the limited air movement and higher effective temperature in the animal-occupied zone.

Author Contributions: Conceptualization, X.W. and M.C.; methodology, Q.Y., T.A. and G.Z.; software, X.W. and M.C.; validation, X.W. and M.C.; formal analysis, X.W. and M.C.; investigation, X.W., M.C. and F.H.; resources, T.X.; data curation, X.W. and F.H.; writing—original draft preparation, X.W. and M.C.; writing—review and editing, Q.Y., T.A., D.J. and G.Z.; visualization, M.C.; supervision, K.W.; project administration, K.W.; funding acquisition, K.W. All authors have read and agreed to the published version of the manuscript.

Funding: This work was supported by the National Key R&D Program of China (No. 2021YFD2000801) and Zhejiang Provincial Department of Agriculture and Rural Affairs (No. 2021SNLF0).

Institutional Review Board Statement: Not applicable.

Informed Consent Statement: Not applicable.

Data Availability Statement: Not applicable.

Acknowledgments: The authors appreciated the help from the engineers in the pig farm during field experiments.

Conflicts of Interest: The authors declare no conflict of interest.

References

1. Wang, X.; Wu, J.; Yi, Q.; Zhang, G.; Amon, T.; Janke, D.; Li, X.; Chen, B.; He, Y.; Wang, K. Numerical evaluation on ventilation rates of a novel multi-floor pig building using computational fluid dynamics. *Comput. Electron. Agric.* **2021**, *182*, 106050. [CrossRef]
2. Baxter, E.M.; Adeleye, O.O.; Jack, M.C.; Farish, M.; Ison, S.H.; Edwards, S.A. Achieving optimum performance in a loose-housed farrowing system for sows: The effects of space and temperature. *Appl. Anim. Behav. Sci.* **2015**, *169*, 9–16. [CrossRef]
3. Spoolder, H.A.M.; Aarnink, A.A.J.; Vermeer, H.M.; van Riel, J.; Edwards, S.A. Effect of increasing temperature on space requirements of group housed finishing pigs. *Appl. Anim. Behav. Sci.* **2012**, *138*, 229–239. [CrossRef]
4. Ecim-Djuric, O.; Topisirovic, G. Energy efficiency optimization of combined ventilation systems in livestock buildings. *Energy Build.* **2010**, *42*, 1165–1171. [CrossRef]
5. Saha, C.K.; Zhang, G.; Ni, J.-Q.; Ye, Z. Similarity criteria for estimating gas emission from scale models. *Biosyst. Eng.* **2011**, *108*, 227–236. [CrossRef]
6. Gao, Y.; Diao, Y.; Lin, C.; Liu, Y.; Guo, C.; Lei, M.; Tong, Y.; Li, X. Monitoring and analysis of thermal environment and harmful gases in mechanically ventilated multistory pig buildings. *Trans. Chin. Soc. Agric. Eng.* **2018**, *34*, 239–247. (In Chinese)
7. Wang, X.; Li, J.; Wu, J.; Yi, Q.; Wang, X.; Wang, K. Numerical Simulation of the Placement of Exhaust Fans in a Tunnel-Ventilated Layer House During the Fall. *Trans. ASABE* **2021**, *64*, 1955–1966. [CrossRef]
8. Mondaca, M.D.; Choi, C.Y. A Computational Fluid Dynamics Model of a Perforated Polyethylene Tube Ventilation System for Dairy Operations. *Trans. ASABE* **2016**, *59*, 1585–1594.
9. Qin, C.; Wang, X.; Zhang, G.; Yi, Q.; He, Y.; Wang, K. Effects of the slatted floor layout on flow pattern in a manure pit and ammonia emission from pit-A CFD study. *Comput. Electron. Agric.* **2020**, *177*, 105677. [CrossRef]
10. Rong, L.; Aarnink, A.J.A. Development of ammonia mass transfer coefficient models for the atmosphere above two types of the slatted floors in a pig house using computational fluid dynamics. *Biosyst. Eng.* **2019**, *183*, 13–25. [CrossRef]
11. Wang, X.; Zhang, G.; Choi, C.Y. Evaluation of a precision air-supply system in naturally ventilated freestall dairy barns. *Biosyst. Eng.* **2018**, *175*, 1–15. [CrossRef]
12. Yeo, U.-H.; Lee, I.-B.; Kim, R.-W.; Lee, S.-Y.; Kim, J.-G. Computational fluid dynamics evaluation of pig house ventilation systems for improving the internal rearing environment. *Biosyst. Eng.* **2019**, *186*, 259–278. [CrossRef]
13. Yi, Q.; Janke, D.; Thormann, L.; Zhang, G.; Amon, B.; Hempel, S.; Nosek, Š.; Hartung, E.; Amon, T. Airflow Characteristics Downwind a Naturally Ventilated Pig Building with a Roofed Outdoor Exercise Yard and Implications on Pollutant Distribution. *Appl. Sci.* **2020**, *10*, 4931. [CrossRef]
14. Zhou, B.; Wang, X.; Mondaca, M.R.; Rong, L.; Choi, C.Y. Assessment of optimal airflow baffle locations and angles in mechanically-ventilated dairy houses using computational fluid dynamics. *Comput. Electron. Agric.* **2019**, *165*, 104930. [CrossRef]
15. Patankar, S. *Numerical Heat Transfer and Fluid Flow*; CRC Press: Washington, DC, USA; Hemisphere Publishing Corp.: Washington, DC, USA, 1980; p. 210.
16. Bjerg, B.; Cascone, G.; Lee, I.-B.; Bartzanas, T.; Norton, T.; Hong, S.-W.; Seo, I.-H.; Banhazi, T.; Liberati, P.; Marucci, A.; et al. Modelling of ammonia emissions from naturally ventilated livestock buildings. Part 3: CFD modelling. *Biosyst. Eng.* **2013**, *116*, 259–275. [CrossRef]
17. Norton, T.; Grant, J.; Fallon, R.; Sun, D.-W. Optimising the ventilation configuration of naturally ventilated livestock buildings for improved indoor environmental homogeneity. *Build. Environ.* **2010**, *45*, 983–995. [CrossRef]
18. Rojano, F.; Bournet, P.-E.; Hassouna, M.; Robin, P.; Kacira, M.; Choi, C.Y. Modelling heat and mass transfer of a broiler house using computational fluid dynamics. *Biosyst. Eng.* **2015**, *136* (Suppl. C), 25–38. [CrossRef]
19. ANSYS Fluent. *Ansys Fluent Theory Guide*; ANSYS Inc.: Canonsburg, PA, USA, 2016.
20. Bjerg, B.; Zhang, G.-Q.; Kai, P. CFD Analyses of Methods to Improve Air Quality and Efficiency of Air Cleaning in Pig Production. In *Chemistry, Emission Control, Radioactive Pollution and Indoor Air Quality*; Mazzeo, N., Ed.; IntechOpen: London, UK, 2011.
21. Baxter, S.H. *Intensive Pig Production: Environmental Management and Design*; Granada Publishing Ltd.: London, UK, 1984; p. 588.
22. CIGR. *Climatization of Animal Houses. Heat and Moisture Production at Animal and House Levels*; Research Centre Bygholm: Horsens, Denmark, 2002.
23. Rong, L.; Pedersen, P.; Jensen, T.L.; Morsing, S.; Zhang, G. Dynamic performance of an evaporative cooling pad investigated in a wind tunnel for application in hot and arid climate. *Biosyst. Eng.* **2017**, *156* (Suppl. C), 173–182. [CrossRef]
24. Deng, S.; Shi, Z.; Li, B.; Zhao, S.; Ding, T.; Zheng, W. CFD simulation of airflow distribution in low profile cross ventilated dairy cattle barn. *Trans. Chin. Soc. Agric. Eng.* **2014**, *30*, 139–146. (In Chinese)
25. BESS Lab. *Final Report #17137*; University of Illinois, Department of Agricultural and Biological Engineering: Urbana, IL, USA, 2017.
26. Bjerg, B.; Rong, L.; Zhang, G. Computational prediction of the effective temperature in the lying area of pig pens. *Comput. Electron. Agric.* **2018**, *149*, 71–79. [CrossRef]

27. Cheng, Q.; Li, H.; Rong, L.; Feng, X.; Zhang, G.; Li, B. Using CFD to assess the influence of ceiling deflector design on airflow distribution in hen house with tunnel ventilation. *Comput. Electron. Agric.* **2018**, *151*, 165–174. [CrossRef]
28. Tabase, R.K.; Van linden, V.; Bagci, O.; De Paepe, M.; Aarnink, A.J.A.; Demeyer, P. CFD simulation of airflows and ammonia emissions in a pig compartment with underfloor air distribution system: Model validation at different ventilation rates. *Comput. Electron. Agric.* **2020**, *171*, 105297. [CrossRef]